CHEMICAL REACTION OF CARBON MONOXIDE WITH COPPER(I)–TETRACHLOROALUMINATE(III)–AROMATIC HYDROCARBON SOLUTIONS
—EQUILIBRIUM AND KINETICS—

TSUNEYUKI SATO, ITSUO TOYODA, YOSHIYUKI YAMAMORI, TOSHIKUNI YONEMOTO, HARUO KATO AND TEIRIKI TADAKI
Department of Chemical Engineering, Tohoku University, Sendai 980

Key Words: Chemical Reaction, Carbon Monoxide, COSORB Solution, Chemical Equilibrium, Reaction Mechanism, Gas Solubility, Complex Stability Constant

Chemical reactions of CO gas with copper(I)–tetrachloroaluminate(III)–aromatic hydrocarbon solutions, namely COSORB solutions, were investigated from the viewpoint of equilibrium and kinetics.

The equilibrium and the non-equilibrium amounts of CO dissolved into COSORB solutions were measured by using a batchwise gas–liquid contactor.

Equilibrium properties such as CO gas solubility constants or CO-complex stability constants for various solvent solutions were determined from the experimental data with the aid of the optimization technique. The solubility of CO decreased with temperature as well as with concentration of $CuAlCl_4$. The stability constants were influenced by the π-electron releasing ability of the aromatic hydrocarbon molecule.

A rational reaction mechanism is proposed to explain the non-equilibrium rate data obtained experimentally. The reaction followed a unimolecular substitution mechanism and was determined to be exothermic. The CO-complex stability constant calculated from the optimum rate constant was in good agreement with the results of the equilibrium experiments.

Introduction

The development of an excellent method of separation and purification of CO gas is a matter of great urgency in C_1 chemistry processes which utilize CO as a starting material for the production of many kinds of chemicals.

There are many well-known methods to separate CO from gaseous mixtures such as cryogenic separation[5] and the ammoniacal copper liquor process.[6] These processes, however, are not attractive for C_1 chemistry because they cannot produce high-purity CO gas economically from refinery or metal furnace off-gas streams.

However, the COSORB process[1,2], which is based on the selective and reversible complexation of CO with $CuAlCl_4$ in an aromatic hydrocarbon solvent, and has a substantial capital advantage over other competing processes, since it produces high-purity CO gas under practical operating conditions.

Regarding the COSORB process, Turner *et al.*[9] clarified the crystal structure of $C_6H_6CuAlCl_4$ by X-ray diffraction techniques. Hirai *et al.*[4] studied the resistance of polystyrene additive against water, which deactivates COSORB solution irreversibly.

Since this process is not well understood, however, we investigated the reaction of CO gas and COSORB solution from the viewpoint of equilibrium and kinetics.

By using equilibrium data, the CO gas solubility constant and CO-complex stability constant were determined. The resulting properties are discussed from the viewpoint of the electronic theory of organic compounds.

A rational reaction mechanism is also proposed to explain the rate data obtained experimentally.

1. Experimental

The apparatus used to measure the equilibrium and the rate of reaction was a modification of Loprest's apparatus[7] and is shown schematically in **Fig. 1**. The characteristic feature of the apparatus is its ability to easily change the partial pressure of CO in the flask.

COSORB solutions were prepared by dissolving CuCl and $AlCl_3$ into an aromatic hydrocarbon solvent and then homogenized by stirring for several hours in a mixing flask. All chemicals used were reagent grade and aromatic solvents were thoroughly dehydrated with sodium sulfate before use. All these procedures were done in a dry box. After being degassed by boiling, the prepared solutions were

Received July 16, 1987. Correspondence concerning this article should be addressed to T. Tadaki. H. Kato is now at Dept. Chem. Eng., Ichinoseki National College of Technology, Ichinoseki 021.

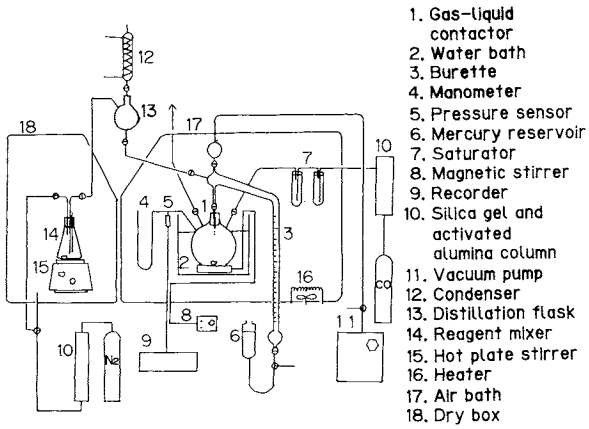

Fig. 1. Schematic diagram of experimental apparatus

stored in a burette.

CO gas from a cylinder was passed through a packed bed of silica gel and a packed bed of activated alumina to remove any traces of water, and then mixed with dry nitrogen. The gas mixture obtained was subsequently saturated with aromatic hydrocarbon solvent vapor. Finally, the gas was introduced to a gas–liquid contactor flask.

After the flask was filled with the prepared gas, a fixed amount of solution was introduced to the flask by mercury overflow. During the reaction period the liquid was agitated by a magnetic stirrer to maintain perfect mixing.

By measuring the small pressure change in the gas–liquid contactor with a manometer or pressure sensor, the reaction could be followed with the aid of the following mass balance equation:

$$n = \Delta P(V - v)/(R \cdot T) \tag{1}$$

Experimental conditions are listed in **Table 1**.

Table 1. Experimental conditions for measuring equilibrium and rate of reaction

Solvent	Benzene, Toluene, *o*-Xylene
Total $CuAlCl_4$ conc.	100–1000 [mol/m^3]
Temperature	274–313 [K]
Partial pressure of CO	5.1×10^3–1.4×10^5 [Pa]

2. Results and Discussion

2.1 Chemical equilibrium between CO and COSORB solution

According to Turner *et al.*,[9] aromatic-$CuAlCl_4$ complex has two tetrahedral structures containing sp^3 hybrid orbitals with respect to each metal atom. Al has four metal-to-chlorine bonds. Cu(I) has three metal-to-chlorine bonds and one metal-to-aromatic ring interaction. Reaction between dissolved CO and COSORB solution may take place with replacement of the lone CO electron pair from the π-electron of the aromatic hydrocarbon molecule.

Overall reaction between dissolved CO and COSORB solution proceeds reversibly as

$$\mathrm{CO(dissolved)} + \mathrm{Ar \cdot X} = \mathrm{CO \cdot X} + \mathrm{Ar} \tag{2}$$

where $\mathrm{X} = CuAlCl_4$ and Ar = aromatic hydrocarbon

By using the equilibrium concentration of each species, the complex stability constant K can be expressed mathematically as follows:

$$K = [\mathrm{CO \cdot X}]_e \cdot [\mathrm{Ar}]_e / ([\mathrm{CO}]_e \cdot [\mathrm{Ar \cdot X}]_e) \tag{3}$$

By assuming Henry's law at the gas–liquid interface and also uniform concentration in the liquid and gas phases, the following relation for the CO molecule can be set up between the gas and liquid phases.

$$[\mathrm{CO}] = H \cdot P_{\mathrm{CO}} \tag{4}$$

Mass balance relations of each species in the liquid phase are given as follows.*1

$$[\mathrm{CO}]_T = [\mathrm{CO}] + [\mathrm{CO \cdot X}] \tag{5}$$

$$[\mathrm{Ar}]_T = [\mathrm{Ar}] + [\mathrm{Ar \cdot X}] \tag{6}$$

$$[\mathrm{X}]_T = [\mathrm{Ar \cdot X}] + [\mathrm{CO \cdot X}] \tag{7}$$

Thus, an explicit expression for the total concentration of CO in the liquid phase can be derived from Eqs. (3) to (7):

$$[\mathrm{CO}]_T = H \cdot P_{\mathrm{CO},e} + 0.5\{\sqrt{([\mathrm{Ar}]_T - [\mathrm{X}]_T + K \cdot H \cdot P_{\mathrm{CO},e})^2 + 4K \cdot H \cdot [\mathrm{X}]_T \cdot P_{\mathrm{CO},e}} - ([\mathrm{Ar}]_T - [\mathrm{X}]_T - K \cdot H \cdot P_{\mathrm{CO},e})\} \tag{8}$$

Figure 2 shows the concentration of CO dissolved in various COSORB solutions under equilibrium conditions. The ordinate is the total concentration of chemical species containing CO, which is normalized by total $CuAlCl_4$ concentration. The solid lines in the figure represent the results obtained by using estimated equilibrium parameters. The details of the estimation will be discussed in a later section. From the experimental results, it can be seen that equilibrium amount of absorption is greatest when benzene is used as a solvent and smallest when *o*-xylene is used. The order of the uptake capability of CO is consistent with the result of Hirai *et al.*[4] obtained by the gas burette method.

*1 A large portion of $CuAlCl_4$ is solvated by forming a stable coordination compound in a COSORB solution.[9] So the concentration of free $CuAlCl_4$, [X], can be omitted in the material balance Eq. (7).

Table 2. H and K for various COSORB solutions

	Total $CuAlCl_4$ conc. [mol/m^3]	Temp. [K]	$H \times 10^6$ [mol/(m^3·Pa)]	$K \times 10^{-4}$ (equilibrium exp.) [—]	Ionization potential [eV]	$K \times 10^{-4}$ (kinetic model) [—]
Toluene	1000	303	8.63	1.52		—
	1000	313	5.51	1.45		—
	100	303	8.51	1.62		—
	100	293	13.32	1.74	9.18	1.77
	100	283	21.51	1.87		1.86
	100	274	32.67	2.00		2.16
	0 (exp.)	303	69.87	—		—
	0 (ref.[8])	303	71.65	—		—
Benzene	1000	303	15.10	2.13		2.14
	100	303	17.17	2.03	9.56	—
	0 (ref.[8])	303	72.24	—		—
o-Xylene	1000	303	7.30	1.40	9.04	—

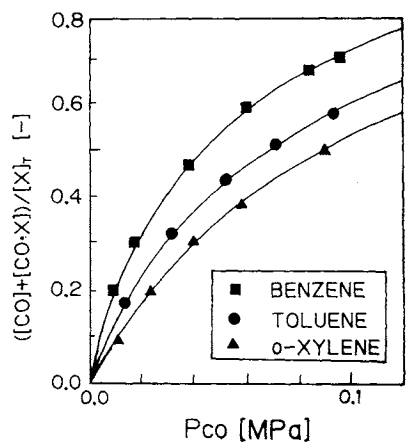

Fig. 2. Effect of solvent species on equilibrium amount of CO dissolved ($[CuAlCl_4]_T = 100$ mol/m^3; $T = 303$ K)

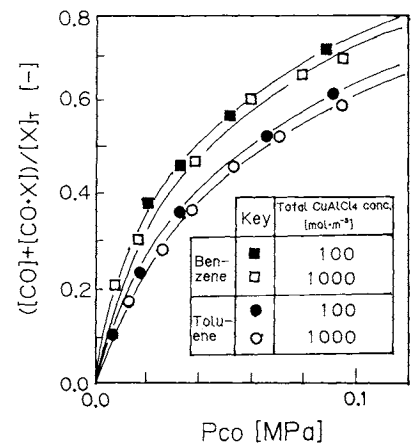

Fig. 3. Effect of total $CuAlCl_4$ concentration on equilibrium amount of CO dissolved ($T = 303$ K)

Figure 3 shows the effect of total $CuAlCl_4$ concentration on the uptake capability at 303 K when benzene or toluene is used as a solvent. It can be seen that the uptake capability is approximately proportional to total concentration of $CuAlCl_4$.

Figure 4 shows the effect of temperature on the CO-uptake capability. Here, the solvent is toluene and the total concentration of $CuAlCl_4$ is 100 mol/m^3. It can be seen that the uptake capability decreases with temperature.

Table 2 shows the optimum values of gas solubility constant, H, and CO complex stability constant, K, obtained by fitting Eq. (8) to experimental data by the Marquardt method.[3] All solid lines in Figs. 2 to 4 are calculated by using optimum H and K and show good agreement with the experimental results.

The solubility of CO for pure solvents,[8] benzene and toluene,[*2] are also listed in Table 2. Compared to these values, the resulting values for COSORB solutions are found to be much smaller.

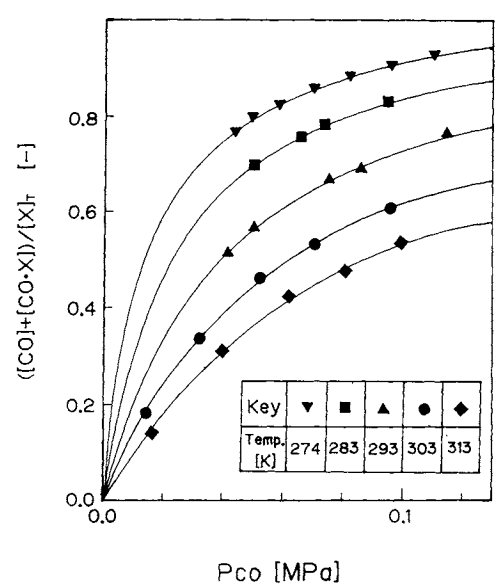

Fig. 4. Effect of temperature on equilibrium amount of CO dissolved (Solvent = Toluene; $[CuAlCl_4]_T = 100$ mol/m^3)

The gas solubility constant in the COSORB solution is greatest when the solvent is benzene and smallest when the solvent is *o*-xylene. This order is the

[*2] For toluene, the Henry constant was also determined experimentally to check the validity of the experiment.

same for the complex stability constant.

The results for K can be explained on the basis of the ionization potential of each solvent. The values are also shown in Table 2. Thus, the larger the ionization potential of aromatic molecule, the smaller is the affinity of the aromatic ring for Cu(I) atom in $CuAlCl_4$ complex. In this situation, it is easy for the lone CO electron pair to coordinate with the Cu(I) atom.

2.2 Determination of reaction mechanism and estimation of kinetic constants

Since the overall reaction shown in Eq. (2) is a substitution reaction of the aromatic ring π-electrons with the lone CO electron pair, there are two probable reaction mechanisms.

One is a unimolecular substitution mechanism as follows:

$$\mathrm{Ar\cdot X} \underset{k_{-1}}{\overset{k_1}{\rightleftharpoons}} \mathrm{Ar+X} \tag{9}$$

$$\mathrm{X+CO} \underset{k_{-2}}{\overset{k_2}{\rightleftharpoons}} \mathrm{CO\cdot X} \tag{10}$$

The reaction starts with low-speed formation of dissociated intermediate, X, and terminates by the fast association of the intermediate with CO. This reaction sequence will be referred to as a SN1 type mechanism hereinafter.

The other is a bimolecular substitution reaction mechanism as follows:

$$\mathrm{Ar\cdot X+CO} \underset{k_{-3}}{\overset{k_3}{\rightleftharpoons}} \mathrm{Ar\cdot X\cdot CO} \tag{11}$$

$$\mathrm{Ar\cdot X\cdot CO} \underset{k_{-4}}{\overset{k_4}{\rightleftharpoons}} \mathrm{CO\cdot X+Ar} \tag{12}$$

This scheme starts with low-speed formation of associated intermediate of $Ar\cdot X\cdot CO$ and terminates by fast decomposition of the intermediate to $CO\cdot X$ and Ar. This sequence will be referred to as a SN2 type mechanism.

Now by considering that reactions proceed in a batchwise gas–liquid contactor, the overall rates of reaction are expressed as follows for SN1 and SN2 type mechanisms, respectively. (See **Appendix**):

$$r=-\frac{d[\mathrm{Ar\cdot X}]}{dt}=\frac{k_1k_2[\mathrm{CO}]+k_{-1}k_{-2}[\mathrm{Ar}]}{k_2[\mathrm{CO}]+k_{-1}[\mathrm{Ar}]}\{[\mathrm{Ar\cdot X}]-[\mathrm{Ar\cdot X}]_e\} \tag{13}$$

$$r=-\frac{d[\mathrm{Ar\cdot X}]}{dt}=\frac{k_3k_4[\mathrm{CO}]+k_{-3}k_{-4}[\mathrm{Ar}]}{k_4+k_{-3}}\{[\mathrm{Ar\cdot X}]-[\mathrm{Ar\cdot X}]_e\} \tag{14}$$

Either of the above equations can be rewritten as follows:

$$r=-\frac{d[\mathrm{Ar\cdot X}]}{dt}=\alpha([\mathrm{Ar\cdot X}]-[\mathrm{Ar\cdot X}]_e) \tag{15}$$

where α are defined as Eqs. (16) and (17), respectively.

$$\alpha_{SN1}=\frac{k_1P_{CO}+(k_{-1}k_{-2}/k_2)[\mathrm{Ar}]/H}{P_{CO}+(k_{-1}/k_2)[\mathrm{Ar}]/H} \tag{16}$$

$$\alpha_{SN2}=\frac{k_3k_4HP_{CO}+k_{-3}k_{-4}[\mathrm{Ar}]}{k_4+k_{-3}} \tag{17}$$

α can be regarded as constant*3 by considering that the amount of an aromatic solvent is in excess compared to that of any other species and further that the concentration change of CO in the liquid phase during the reaction period is negligibly small.

A quantitative calculation based on the theory of gas–liquid mass transfer with chemical reaction[10] indicates that the mass transfer resistance is negligible under our experimental conditions.

Now, integrating Eq. (15) under the following initial condition,

$$[\mathrm{Ar\cdot X}]|_{t=0}=[\mathrm{Ar\cdot X}]_0 \tag{18}$$

the result is

$$\alpha\cdot t=\ln\frac{[\mathrm{Ar\cdot X}]_0-[\mathrm{Ar\cdot X}]_e}{[\mathrm{Ar\cdot X}]-[\mathrm{Ar\cdot X}]_e}(\equiv Y) \tag{19}$$

Experimentally, $[Ar\cdot X]$ can be obtained from ΔP by using the following mass balance relation:

$$[\mathrm{Ar\cdot X}]=[\mathrm{Ar\cdot X}]_0-\Delta P(V-v)/(R\cdot T\cdot v)+H\cdot P_{CO} \tag{20}$$

Reaction time t should be proportional to Y of Eq. (19), provided that the reaction proceeds by SN1 or SN2 type mechanism.

Figure 5 shows the results obtained under the conditions of various temperatures and partial pressures of CO using toluene as a solvent. A linear relationship exists at every temperature. It can also be seen that α increases with the CO partial pressure.

According to Eqs. (16) to (17), α should have a different dependence on P_{CO}.

As indicated by **Fig. 6**, the reaction proceeds by the SN1 mechanism.

Solid lines are the calculated results for the SN1 mechanism with the optimum kinetic parameters obtained by Marquardt's method. All lines are in good agreement with experimental data.

By using the following relation,

*3 Since P_{CO} decreased only about 7% with time during the reaction period, the change of P_{CO} can be ignored for the calculation of α.

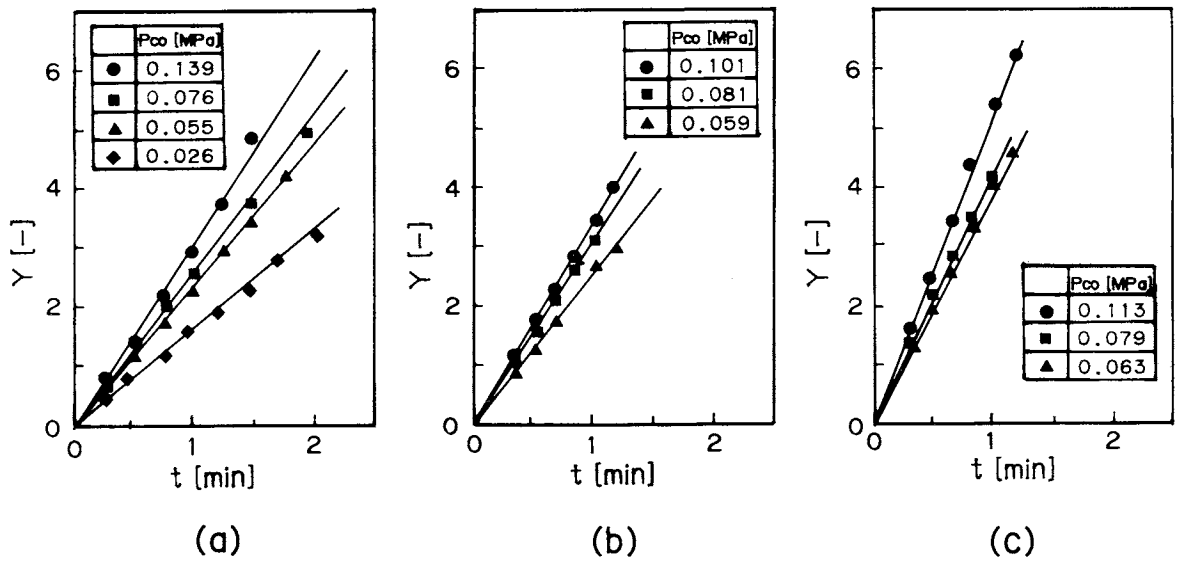

Fig. 5. Variations of Y with time for various P_{co} ($[CuAlCl_4]_T = 100\,mol/m^3$; (a): $T = 274\,K$; (b): $T = 283\,K$; (c): $T = 293\,K$)

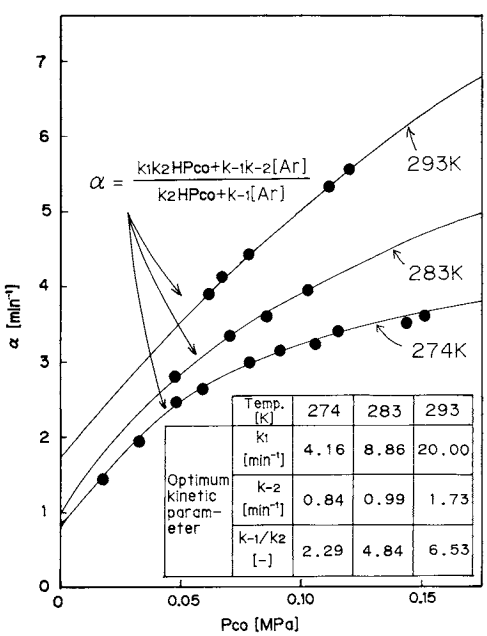

Fig. 6. Relationship between α and P_{co} based on SN1 type mechanism ($[Ar] = 9400\,mol/m^3$)

$$K\left(=\frac{[Ar]_e \cdot [CO \cdot X]_e}{[Ar \cdot X]_e \cdot [CO]_e}\right)=\frac{k_1 k_2}{k_{-1}k_{-2}} \qquad (21)$$

values of the complex stability constant K were calculated from the kinetic parameters and are listed in the right-hand column of Table 2. They are in good agreement with the results of equilibrium experiments. The complex, $CuAlCl_4$, has a chain-link structure possessing a tetrahedral framework. The SN1 mechanism without the formation of a 5-coordinated intermediate is thought to be stereochemically more likely than the SN2 mechanism with the formation of a 5-coordinated intermediate.

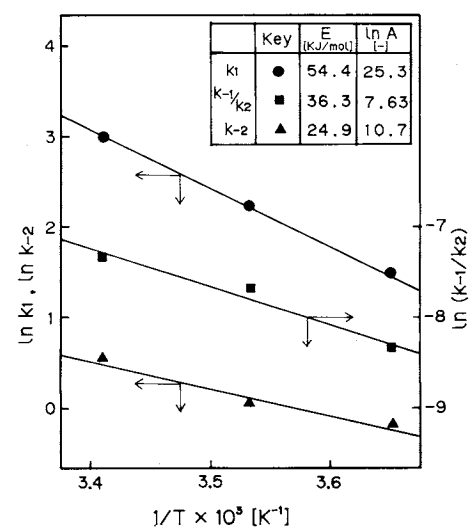

Fig. 7. Arrhenius plot for k_1, k_{-2}, k_{-1}/k_2

Figure 7 shows the Arrhenius plots of the kinetic parameters, k_1, k_{-2} and k_{-1}/k_2. Each plot gives almost a straight line.

Figure 8 shows the energy variation of the reaction schematically. From the figure, the overall heat of reaction can be calculated as

$$\Delta H = -E_{-2} - (E_{-1} - E_2) + E_1 = -6.8\,KJ/mol$$

which indicates an exothermic reaction.

Conclusion

Investigation of the chemical reaction process of CO with COSORB solutions was made, leading to the following conclusions:

The equilibrium amount of CO dissolved varied with temperature, pressure P_{CO} and solvent and was proportional to $[CuAlCl_4]_T$.

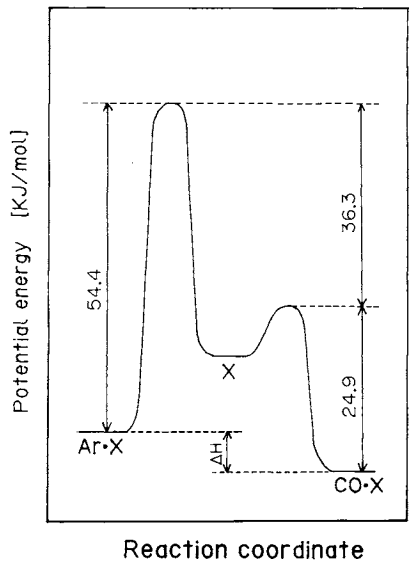

Fig. 8. Energy variation for SN1 type mechanism

CO gas solubility constant and CO-complex stability constant were obtained for various solvent solutions by an optimization technique. The solubility of CO decrease with temperature and with total concentration of $CuAlCl_4$. The complex stability constant was influenced by the π-electron releasing ability of the aromatic hydrocarbon molecule.

The reaction followed a unimolecular substitution mechanism and was determined to be exothermic. The CO-complex stability constant was in good agreement with the results obtained in equilibrium experiments.

Appendix

Derivation of Eqs. (13) and (14).

For an isothermal, constant-volume batch gas-liquid contactor, the rate of reaction of Ar·X and X for SN1 type mechanism can be written as follows:

$$-\frac{d[\mathrm{Ar}\cdot\mathrm{X}]}{dt}=k_1[\mathrm{Ar}\cdot\mathrm{X}]-k_{-1}[\mathrm{Ar}][\mathrm{X}] \tag{A-1}$$

$$\frac{d[\mathrm{X}]}{dt}=k_1[\mathrm{Ar}\cdot\mathrm{X}]-k_{-1}[\mathrm{Ar}][\mathrm{X}]-k_2[\mathrm{CO}][\mathrm{X}]+k_{-2}[\mathrm{CO}\cdot\mathrm{X}] \tag{A-2}$$

Applying the quasi-steady state hypothesis to the intermediate, X, gives

$$[\mathrm{X}]=\frac{k_1[\mathrm{Ar}\cdot\mathrm{X}]+k_{-2}[\mathrm{CO}\cdot\mathrm{X}]}{k_{-1}[\mathrm{Ar}]+k_2[\mathrm{CO}]} \tag{A-3}$$

Substituting the above equation into Eq. (A-1) yields the following equation.

$$-\frac{d[\mathrm{Ar}\cdot\mathrm{X}]}{dt}=\frac{k_1k_2[\mathrm{Ar}\cdot\mathrm{X}][\mathrm{CO}]-k_{-1}k_{-2}[\mathrm{Ar}][\mathrm{CO}\cdot\mathrm{X}]}{k_{-1}[\mathrm{Ar}]+k_2[\mathrm{CO}]} \tag{A-4}$$

Further, mass balance requirement for species X gives the following relation.

$$[\mathrm{CO}\cdot\mathrm{X}]=[\mathrm{Ar}\cdot\mathrm{X}]_0-[\mathrm{Ar}\cdot\mathrm{X}]-[\mathrm{X}] \tag{A-5}$$

Under the assumption of negligibly small [X], Eqs. (A-4) and (A-5) can be manipulated to yield

$$-\frac{d[\mathrm{Ar}\cdot\mathrm{X}]}{dt}=\frac{k_1k_2[\mathrm{CO}]+k_{-1}k_{-2}[\mathrm{Ar}][\mathrm{Ar}\cdot\mathrm{X}]}{k_{-1}[\mathrm{Ar}]+k_2[\mathrm{CO}]}+\frac{k_{-1}k_2[\mathrm{Ar}][\mathrm{Ar}\cdot\mathrm{X}]_0}{k_{-1}[\mathrm{Ar}]+k_2[\mathrm{CO}]} \tag{A-6}$$

At equilibrium, the net reaction rate is zero, and the following relation can be obtained from Eq. (A-6).

$$k_{-1}k_{-2}[\mathrm{Ar}]_e\cdot[\mathrm{Ar}\cdot\mathrm{X}]_0=-\{k_1k_2[\mathrm{CO}]_e+k_{-1}k_{-2}[\mathrm{Ar}]_e\}[\mathrm{Ar}\cdot\mathrm{X}]_e \tag{A-7}$$

Finally, substituting Eq. (A-7) into Eq. (A-6) yields Eq. (13) for a unimolecular substitution reaction mechanism.

For a bimolecular substitution reaction mechanism, the rates of reaction of Ar·X and Ar·X·CO are given as follows:

$$-\frac{d[\mathrm{Ar}\cdot\mathrm{X}]}{dt}=k_3[\mathrm{Ar}\cdot\mathrm{X}][\mathrm{CO}]-k_{-3}[\mathrm{Ar}\cdot\mathrm{X}\cdot\mathrm{CO}] \tag{A-8}$$

$$-\frac{d[\mathrm{Ar}\cdot\mathrm{X}\cdot\mathrm{CO}]}{dt}=k_3[\mathrm{Ar}\cdot\mathrm{X}][\mathrm{CO}]-k_{-3}[\mathrm{Ar}\cdot\mathrm{X}\cdot\mathrm{CO}]-k_4[\mathrm{Ar}\cdot\mathrm{X}\cdot\mathrm{CO}]+k_{-4}[\mathrm{Ar}][\mathrm{CO}\cdot\mathrm{X}] \tag{A-9}$$

Applying the quasi-steady state hypothesis to the intermediate, Ar·X·CO, Eq. (14) can finally be derived.

Acknowledgment

This research was supported in part by a Grant-in-Aid for Scientific Research "Special Project Research on Energy (Energy (1))" of the Ministry of Education, Japan, 1981–1986.

Nomenclature

$E_i(i=1, 2, -1, -2)$	= activation energy	[kJ/mol]
H	= gas solubility coefficient	[kmol/(m³·Pa)]
ΔH	= heat of reaction	[kJ/mol]
K	= complex stability const. defined by Eq. (3)	[—]
$k_i(i=1, 4, -2, -3)$	= rate const. of elementary reactions	[1/min]
$k_i(i=2, 3, -1, -4)$	= rate const. of elementary reactions	[m³/(mol·min)]
n	= amount of reaction	[mol]
P	= pressure	[Pa]
ΔP	= pressure difference	[Pa]
R	= gas constant	[Pa·m³/(mol·K)]
r	= reaction rate	[kmol/(m³·min)]
T	= temperature	[K]
t	= time	[min]
V	= total flask volume	[m³]
v	= charged volume of COSORB solution	[m³]
Y	= right-had side of Eq. (19)	[—]
[ ]	= liquid-phase concentration	[mol/m³]
α	= parameter defined by Eqs. (16) or (17)	[1/min]

〈Subscripts〉

e	= equilibrium state
0	= initial value

Literature Cited

1) Haase, D. J. and D. G. Walker: *Chem. Eng. Prog.*, **70**, 74 (1974).
2) Haase, D. J.: *Chemical Engineering*, **82**, Aug., 52 (1975).

3) Henry, E. J. and E. M. Rosen: "Material and Energy Balance Computations," p. 202, Wiley, New York (1969).
4) Hirai, H., M. Komiyama and S. Hara: *Makromol. Chem. Rapid Commun.*, **2**, 495 (1981).
5) Kitagawa, H. and A. Inoue: *Nenryou Kyoukaishi*, **45**, 110 (1966).
6) Larson, A. T. and C. S. Teithworth: *J. Am. Chem. Soc.*, **44**, 2878 (1922).
7) Loprest, F. J.: *J. Phys. Chem.*, **61**, 1128 (1957).
8) Stephen, H. and T. Stephen: "Solubilities of Inorganic and Organic Compounds," Vol. 1, Part 2, p. 1053, Pergamon Press (1963).
9) Turner, R. W. and E. L. Amma: *J. Am. Chem. Soc.*, **88**, 187 (1966).
10) Westerterp, K. R., W. P. M. van Swaaij and A. A. C. M Beenackers: "Chemical Reactor Design and Operation", 2nd ed., p. 377, Wiley, New York (1984).

(Presented at Hokkaido Meeting of The Society of Chemical Engineers, Japan at Sapporo, July, 1987.)

EFFECT OF ANODIC AND CATHODIC REACTIONS ON OXIDATIVE DEGRADATION OF PHENOL IN AN UNDIVIDED BIPOLAR ELECTROLYZER

MASAO SUDOH, TAKAMASA KODERA, HARUYOSHI HINO AND HIROSHI SHIMAMURA

Department of Chemical Engineering, Shizuoka University, Hamamatsu 432

Key Words: Electrolysis, Bipolar Electrode, Oxidative Degradation, Phenol, Current Efficiency

Both anodic oxidation and generation of hydrogen peroxide through electroreduction of oxygen may be useful for oxidative degradation of organic compounds. To clarify the effect of electrode reactions of both sides of a bipolar plate on the current efficiency for oxidative degradation of phenol, experiments were conducted by using an undivided bipolar electrolyzer having a vertical stack of perforated graphite electrodes. The Faradaic current I_f was arranged as a function of the electrode potential difference E_B between opposite sides of a bipolar plate. By analyzing the $I_f - E_B$ curves for the electrolyses in solutions containing different reactants, separate currents corresponding to anodic and cathodic reactions were determined. The effect of E_B on the COD current efficiency *Ce*(COD) for the oxidative degradation of phenol could be well explained by the contribution of the currents of phenol oxidation and oxygen reduction to the total current. The value of *Ce*(COD) in case of sparging oxygen showed a bimodal curve having the maximum values with respect to E_B.

Introduction

Electrochemical treatments of waste water containing organic compounds are classified into two groups: direct oxidation on the anode and indirect oxidation using an oxidizing agent, hypochlorite[2] or hydrogen peroxide, which is produced by electrolysis.[5] Hydrogen peroxide is produced through electroreduction of oxygen on the cathode.[7,8] In our previous paper,[9] the oxidative degradation of aqueous phenol effluent with electrogenerated Fenton's reagent in a catholyte compartment separated by a membrane in an H-type cell was reported. In the ideal case, both anodic oxidation and cathodic reduction in an undivided cell may be useful for oxidative degradation.

Received July 30, 1987. Correspondence concerning this article should be addressed to M. Sudoh. T. Kodera is now at Nippon Steel Corp. Ltd., Tokai 476.

In the present work, a divided bipolar electrolyzer having a vertical stack of perforated graphite electrodes is used experimentally to clarify the effect of both electrode reactions on total current efficiency for the oxidative degradation of phenol. The current-voltage curves of the electrolysis in solutions containing different reactants are analyzed by use of an equivalent circuit model of a bipolar electrolyzer. The current corresponding to separate electrode reaction on the anodic or cathodic side of a bipolar plate is determined and the contribution of the currents connected with the oxidative degradation to the total current is discussed.

1. Experimental

The bipolar electrolyzer shown in **Fig. 1**, similar to the previous one,[6] was an acrylic cylindrical column 46 mm in inner diameter and 420 mm in height. As